Review of Fission Fragment Propulsion

Pierce M. Jackson
Department of Aerospace Engineering, Auburn University, Auburn, AL, 36849

Dusty Plasma Fission Fragment Rocket Engines directly expel the fission products of nuclear reactions at speeds a few percent the speed of light to produce thrust. Such reactions could realistically obtain specific impulse over 500,000 sec, though with thrust less than 100 N. However, the inclusion of an afterburner could increase thrust to over 4600 N at the cost of reducing specific impulse to 32,000 sec. The products of the fissile fuel could also be used for generating electricity for the spacecraft it is propelling. A spacecraft propelled by an afterburner-configured dusty plamsa fission fragment rocket engine could travel to Saturn and back in 15 years while requiring less than 300 kg of Americium-242m nuclear fuel and approximately 137 metric tons of H_2. In practice, this propulsion system is somewhere between nuclear thermal and nuclear electric, as it can be throttled to heat a working fluid or just expel the fission fragments unimpeded. Much of the technology required to develop a FFRE exists, though one has never been engineered or prototyped. The primary limiting factors are thermal management of the reactor core and the abundance of Americium-242m.

I. Nomenclature

NTP	=	nuclear thermal propulsion
NEP	=	nuclear electric propulsion
FFRE	=	fission fragment rocket engine
FF	=	fission fragments
NIAC	=	NASA Innovative Advanced Concepts
DEC	=	direct energy conversion
HOPE	=	Human Outer Planet Exploration mission
KSP	=	Kerbal Space Program
KSPTOT	=	Kerbal Space Program Trajectory Optimization Tool
Z	=	elemental atomic number
I_{sp}	=	specific impulse
c	=	speed of light
g_0	=	Earth standard gravity
v_{ff}	=	velocity of fission fragment
m_{ff}	=	mass of fission fragment
m_e	=	mass of the FFRE
F_t	=	thrust force of engine
P_{jr}	=	jet power of reactor
$\dot{m}$	=	mass flow rate of fission fragments
a_e	=	acceleration of FFRE
Δv	=	change in velocity for a spacecraft maneuver
m_0	=	spacecraft mass before engine burn
m_f	=	spacecraft mass after engine burn

II. Introduction

Like with nuclear thermal (NTP) and nuclear electric propulsion (NEP), fission fragment rocket engines (FFRE) aim to exploit the energy released via nuclear fission as a means to produce thrust. However, unlike NTP and NEP, FFRE removes the 'middle-man' from the process of thrust generation. NTP uses the energy from nuclear fission to heat and expand a propellant fluid, usually liquid hydrogen, and expel it through a nozzle to generate thrust. NEP converts the nuclear fission energy into electricity which creates thrust by accelerating ions away from the engine at high speeds.

Instead, FFRE induces thrust by directly discharging the products of nuclear fission – the fission fragments – out of the engine. Unhindered, fission fragments can be propelled away from the parent reaction at speeds a few percent the speed light, resulting in extremely high values of specific impulse (I_{sp}), but low thrust because of the low mass flux of the fragments. The engine can be optimized to trade specific impulse for thrust in a similar fashion as NTP resulting in thrust and I_{sp} values in the thousands of newtons and seconds, respectively.

At first glance, the FFRE might seem like an exotic form of propulsion that is not yet within the realm of technological possibility, like antimatter rockets or warp-drives. While a FFRE has never been physically engineered, much of the technology required to develop one has either already been produced, proven at small scales, or established as viable in literature. Of course, nuclear fission is well understood and harnessed in nuclear power plants across the globe. Because the FFRE is essentially an open nuclear reactor being used as a rocket, many of the necessary components exist – neutron moderators and maintaining criticality of the fuel, protective shielding, superconducting magnets, thermal management systems, and thermoelectric generators, for example. While no new physics or major engineering breakthroughs are required for such an engine to be created, the FFRE has, unfortunately, never been funded beyond academic studies.

A large portion of the research on the viability of FFREs, in its current form, originate from a Phase I NASA Innovative Advanced Concepts (NIAC) study [1] and a few accompanying studies [2, 3]. They investigate many logistical aspects of the engine, its design, fuel, and example mission designs and show that a FFRE is compatible with current technology and known physics. However, the NIAC proposal never progressed beyond Phase I and the primary investigators have retired bringing the progress and advocacy of the FFRE to a screeching halt. Thus, no major developments have occurred in recent years and the concept has seemed to recede into ambiguity among the public and scientific community.

The rest of this manuscript will bring to light the concept and evolution of the FFRE up to its current form and then conduct a basic mission analysis. It should be kept in mind that the FFRE, as a whole, has never progressed beyond academic study into engineering models. This does not imply that it is an unrealistic form of propulsion or that it should not be pursued, but rather that the information presented should be interpreted as theoretical possibility awaiting confirmation via testing.

III. Original Concept

The idea of the fission fragment rocket was first published and pursued by George Chapline of Lawrence Livermore National Laboratory in 1988 [4–6]. The original concept was to coat thin fibers (diamerter < 5 μm) with a layer of fissile material and rotate them through a reactor core such that when they entered the core, they will attain criticality and produce fission fragments (see Fig. 1). Because of the thin fibers and thin layer of fuel, the fragments are likely to escape and could then be guided to the rocket exhaust via magnetic fields. However, not all fragments will escape the fibers which will result in a buildup of thermal energy. For reference, the distance travelled by a fission fragment at room temperature and pressure is approximately 2 cm, though the distance they travel within fuel is on the order of micrometers [6, 7]. The disks on which the fibers are situated would quickly rotate out of the core after a brief period of reaching criticality to cool off before re-entering the core. A fuel which achieves criticality at low densities, however, could reduce thermal load on the filaments (because the fragments could more easily escape the fuel) as well as increase the efficiency of the system.

Chapline proposed the use of Curium-245 or the metastable isotope Americium-242m because of their high thermal fission cross-sections and the number of neutrons produced during fission; though he and other studies have shown preference for the latter [5, 6, 8]. The fission cross section by thermal neutrons for ^{242m}Am is approximately 6500 barns and releases an average of 3.6 neurtrons per fission [9] compared to uranium-235's fission cross section of 586 barns and about 2.4 neutrons per fission. Ronen [8] find that for ^{242m}Am, the average range for a fission fragment is ~ 7 μm and that for fuel thickness of less than 1 μm, approximately 90% of the fission product energy directed outward towards the fuel boundary will be capable of escaping the fuel (see Fig. 2). In addition, the large fission cross section implies a lower amount of material required to maintain criticality. For example, assuming a cylindrical core with diameter of 1 meter, length of 5 meters, is uniformly filled with fissile material, and is surrounded by 3 meters of heavy water as a moderator, the critical masses of ^{242m}Am and ^{235}U are 0.41 kg and 11.0 kg, respectively [6, 8].

Ultimately, Chapline imagined an engine that could produce $I_{sp} > 10^6$ seconds; generate around 10 GW of power (depending on the scale of the engine and mission); and with only 50% fission fragment escape probability, propel an interstellar spacecraft to Alpha Centauri in under 150 years.

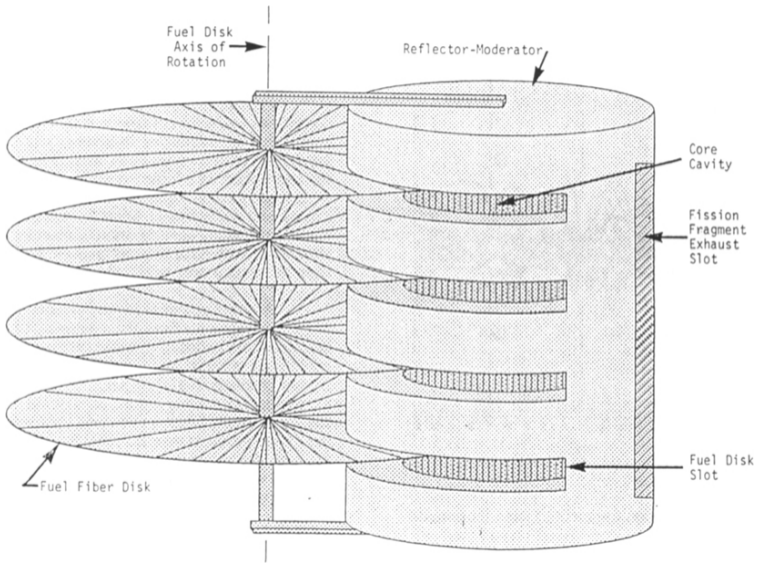

Fig. 1 Schematic of Chapline's fission fragment rocket engine design. Figure taken from [6]

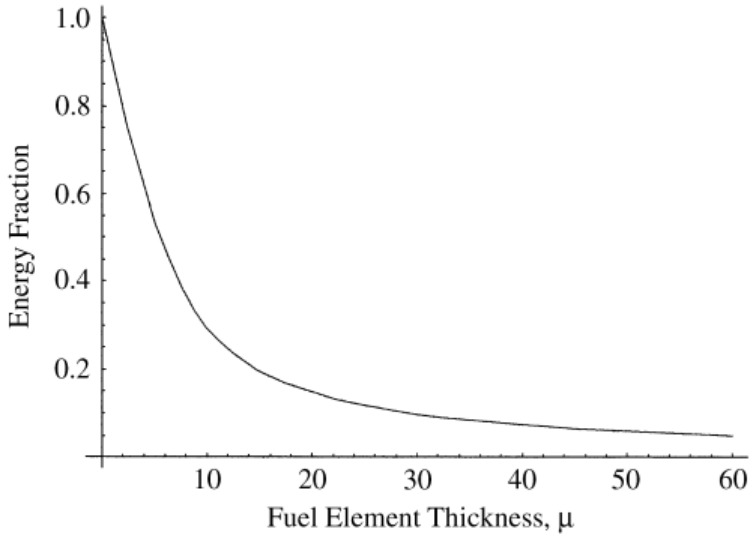

Fig. 2 The fraction of fission energy escaping a given fuel thickness in micron for half of the generated fission fragments. For simplicity, the assumption that a fission event produces two particles of equal mass and equivalent energies directed in opposite directions are made. One particle is assumed to head away from the fuel boundary (that is, towards the moderator) and the other particle is launched towards the boundary indicating the possibility of escaping from the fuel. Thus, this graph represents half the total energy fraction, i.e. the energy fraction of the particles directed towards the boundary that escape. This figure was taken directly from [8]

IV. Dusty Plasma Configuration

In 2005, Rodney Clark and Dr. Rob Sheldon proposed a new, more efficient, and more practical design for nuclear power generation via fission fragments [2]. The basis of their design is to electrostatically confine a cloud of nano-particle fissile material ("dusty plasma") within the core of the reactor. Figure 3a shows a general schematic of a dusty plasma FFRE. This configuration has a variety of benefits over the filament-design.

The small size of the dust particles (i.e. conglomerates of fuel) allows for a high probability of fission fragments escaping the dust particle and entering the dust-cloud as a whole (Fig. 2). Because the dusty plasma is levitated in the core, there is no longer only a single escape-direction as was the case with the fuel-coated carbon filament design. The fuel may fission omni-directionally and the escaped fragments can then be guided via magnetic fields. The magnetic field can be used as a magnetic mirror and direct all fragments, regardless of ejection direction, out of the core to generate thrust. Similarly, fragments could be directed towards a chamber that utilizes direct-energy-conversion (DEC) [10, 11], magnetohydrodynamic conversion, or a Brayton Cycle to produce electrical power for use by the rest of the spacecraft. The strength of the magnetic mirror could be adjusted to prioritize thrust and Isp or electrical power generation.

Additionally, the low density of the plasma and small dust particle size results in a high surface-area to volume ratio and a lower probability of escaped fragments colliding with and heating other dust particles. This can permit sufficient amounts of radiative cooling to maintain equilibrium core temperatures lower than the melting point of the fuel (see Fig. 4). While the temperature of the confined dusty plasma is capable of cooling itself, the heat-shield protecting the walls of the core, surrounding moderator material, and magnets require active cooling.

A. Tuna Can Geometry

Robert Werka worked with Rodney Clark and Dr. Sheldon to further develop the dusty plasma FFRE in a NIAC Phase I investigation. The 'tuna can' geometry they developed (Fig. 3b) maintained much of Clark & Sheldon's original ideas (Fig. 3a). A primary difference is that, instead of utilizing DEC for electricity generation, they use a Brayton Cycle, similar to NEP. To maintain criticality of the low density plasma, a large amount of neutron moderator material is required. Fast neutrons ejected by fission will enter the moderator and re-enter the core multiple times before slowing down to become thermal neutrons which can be captured by the fissile fuel. Because the neutrons make many cycles through the moderator, the material it is made of must have very small neutron capture cross sections; Beryllium, Carbon-13, and deuterium compounds are possibilities. To protect the moderator from the high core temperatures, it is lined with a carbon-carbon heat shield which requires active cooling. In fact, the thermal constraints on the moderator are more stringent than the thermal constraints on the fuel. After absorbing excess heat from the heat shield, coolant flow is passed through a Brayton Cycle engine to generate electricity. A large portion of the energy captured by the heat shield, however, must dumped into space via large radiators.

Similarly, the superconducting magnets that produce the strong magnetic mirror requires active cooling. Additional magnets are used outside of the reactor to form a magnetic nozzle which is used to collimate the fission fragments into a parallel beam away from the engine.

Werka and his team found that, using uranium-dioxide dust as fuel, the initial 'tuna can' FFRE geometry could operate at a power of approximately 1 GW_{th}, fragment exhaust velocity of 1.7 percent the speed of light (I_{sp} = 527,000 sec) and 43 newtons of thrust [1]. These results are listed in Figure 5. It should be noted that, like mentioned previously, a specific impulse on the order of 10^6 seconds is theoretically possible. But, this is with the assumption that fission fragments directly escape the core unhindered. Some fragments do directly escape, but many of them must be redirected by the magnetic mirror and some of those that get redirected will pass back through the dusty plasma cloud. These non-direct paths taken to escape the core result in reduced fragment exit velocities.

B. Half-Torus & Afterburner Configuration

While the 'tuna can' core geometry provided a good starting point for the implementation of the dusty plasma configuration, further neutronic analysis revealed nontrivial issues. Primarily, the exhaust port in the moderator could not be sufficiently large enough for the magnetic bottle to funnel most fragments out while simultaneously being small enough to reflect enough neutrons to maintain criticality in the core. One approach for solving this problem was to develop an entirely new geometry for the FFRE – a half-torus as show in Figure 6.

The new engine geometry fixed the moderator-nozzle hole issue, but changing the shape of the engine also means the changing the shape of the dusty plasma cloud. In the previous design, the cloud was similar to a pancake. For the half-torus, the shape of the cloud changes to something more like a curved cylinder. Werka and his team used the simulation code Geant4 to re-evaluate the neutronics and particle motion within the engine and found that with the new

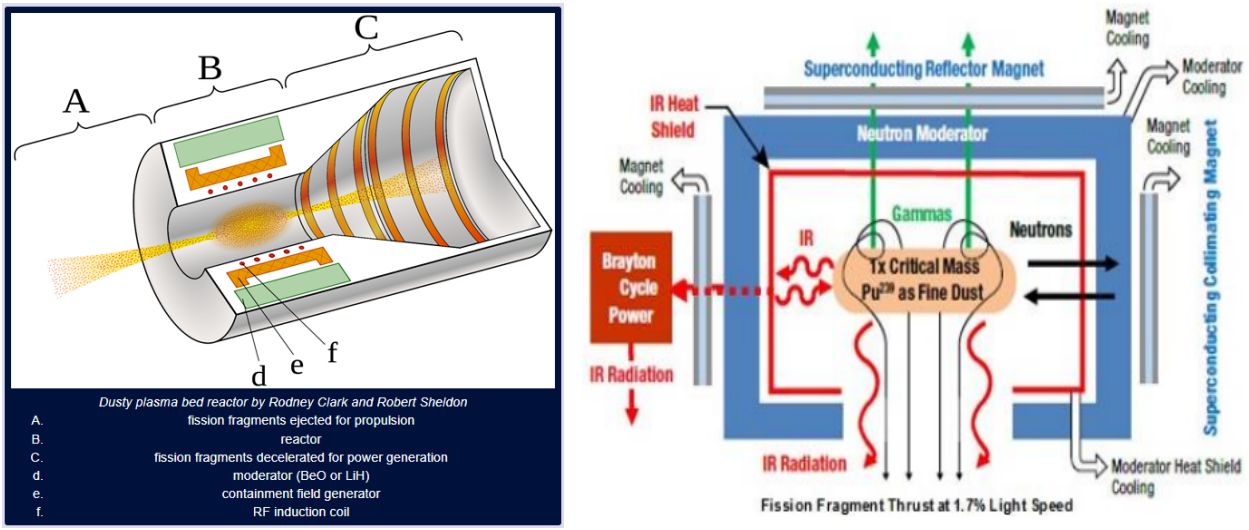

(a) **(b)**

Fig. 3 (a) Schematic of the generation I dusty plasma FFRE design. This design would use direct-energy-conversion in the upper 'C' chamber to generate electricity. Graphic inspired by Figure 2 of [2]. This specific figure was taken directly from [12]. (b) Figure of the core of the engine taken from [1]. This design excludes the upper 'C' chamber and instead opts to use a Brayton Cycle to generate power.

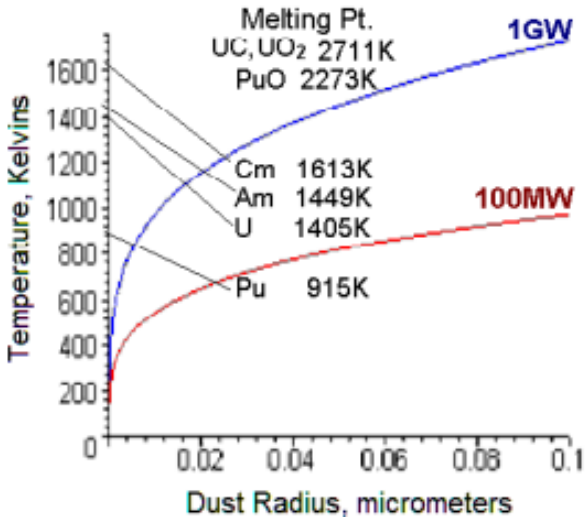

Fig. 4 Dust temperature in the core of the dusty plasma FFRE as a function of dust size. The melting temperatures of various fuels are listed. This figure is taken directly from [2]

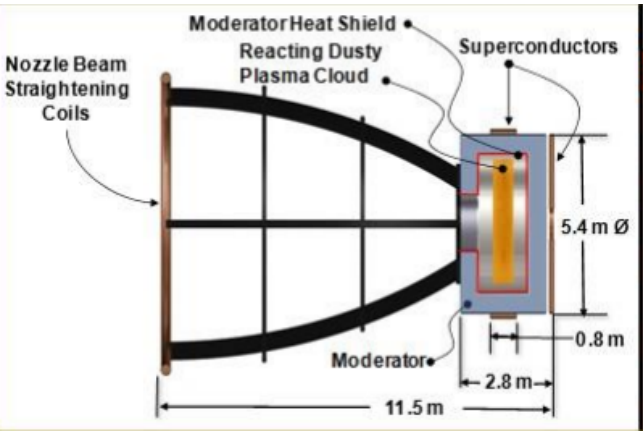

Master Equip List Mass incl 30% MGA	
FFRE System Total, mT	113.4
Nozzle	6.4
Magnetic Mirror	28.6
Exit Field Coil	11.1
Moderator	51.2
Moderator Heat Shield	0.1
Control Drum System	0.7
Electrostatic Collector	0.3
Dust Injector	7.2
Shadow Shield	7.8

Distribution	(MW)
Total Reactor Power	*1,000*
Neutrons (30% to FFRE)	24.2
Gammas (5% to FFRE)	95.6
Other	70.2
Thermal (IR)	699
Jet Power	**111**
Performance	
Thrust	**43 N** (9.7 lbf)
Exit Velocity	**5170 km/s**
Specific Impulse	**527,000 s**
Mass Flow	**0.008 gm/s**

Fig. 5 Results of the 'tuna can' FFRE geometry using uranium dioxide as fuel-dust. The middle panel displays the mass of the FFRE components. Notice that the two most massive components are the moderator and magnets. The third panel, on the right, displays engine performance. The total generated power is 1 GW with 699 MW being heat, most of which is dumped into space via radiators while some is converted to electricity via Brayton Cycle. The specific impulse is an exceptionally high 527,000 seconds, but thrust is a dismal 43 N. The rate that dust in the core must be replenished is approximately 1 ounce per hour. Results and figure taken from [1].

cloud geometry, to maintain sufficient fission fragment escape, the density had to be lowered from 0.1 g cm^{-3} to 0.01 g cm^{-3}. This has the side-effect of lowering the thrust-per-power produced by the engine. Uranium-235 could generate approximately 5 N GW^{-1} with 98% of fission fragments contributing to heat production and only 2% contributing to thrust. Similarly, plutonium-239 generated a similar 5 N GW^{-1} with 97% of fragments going to heat and 3% to thrust. For reference, a thrust-per-power value of 120 N GW^{-1} is considered 'ideal' by the investigation. Recall, however, the properties of Americium-242m. Its massive cross section works well with the now even lower-density plasma and only 60% of fission fragments supply heat and 40% are expelled for thrust resulting in approximately 50 N GW^{-1}.

In this state, the FFRE acts like a large NEP engine with performance similar to the tuna can geometry - high specific impulse, but still low thrust. This is useful for long-duration missions like Chapline imagined to Alpha Centauri, but the closer the mission destination to Earth, the less appealing it becomes. Though, the engine's astronomical I_{sp} can be traded for increased thrust by mass loading, like NTP.

Introducing an 'afterburner' into the engine design, a working fluid (or gas) such as hydrogen can be injected into the flow of expelled fission fragments (see Fig. 7). The kinetic energy of the fragments will heat, ionize, and accelerate the hydrogen gas which will expand and cool to produce greater thrust. The reduction in exhaust particles' velocity implies a reduction in specific impulse, but the increased mass flow increases thrust. This trade-off between Isp and thrust can be adjusted by the amount of mass injected into the fission fragment exhaust beam. This is best explained by the study, itself: "If hydrogen gas flow rate is increased, the fixed power of the fission fragment beam means the final temperature is lower, the exhaust velocity is lower, the mass flow is greater and the thrust is greater as well. Conversely, throttling the hydrogen gas raises the temperature and the final ISP while reducing thrust" [1].

The afterburner requires additional infrastructure. The extended nozzles must maintain their magnetic confinement as before. The 'front' half of the extended nozzle (closest to the reactor) will converge up to the midpoint, where the hydrogen gas is injected. This concentrates the fission fragments for efficient energy transfer to the injected mass. From there, the magnetic nozzle diverges, still guiding the hydrogen away from the engine, but allowing it to expand and cool. Large tanks to store the hydrogen gas must also be added to the engine design.

The FFRE under this afterburner configuration applies properties of both NEP and NTP. As such, it holds a niche position between the two in terms of performance; by controlling the mass flow of the afterburner, performance can be altered to more closely mimic NEP or NTP based on the situation.

V. Technical Analysis

This section will conduct a basic calculation of the FFRE's specific impulse and mass flow rate to obtain thrust originating from the nuclear fission of Americium. Then, an example mission analysis using the afterburner-FFRE will

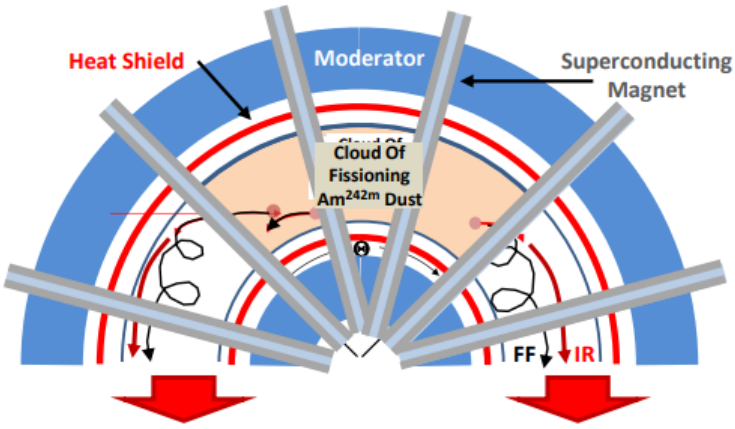

Fig. 6 The FFRE half-torus geometry. In this new design, the two ports of exit double the thrust and the mirror magnet and its heat radiators could be reduced. However, the amount of moderator increases. Ultimately, the acceleration produced by the engine remains unchanged.

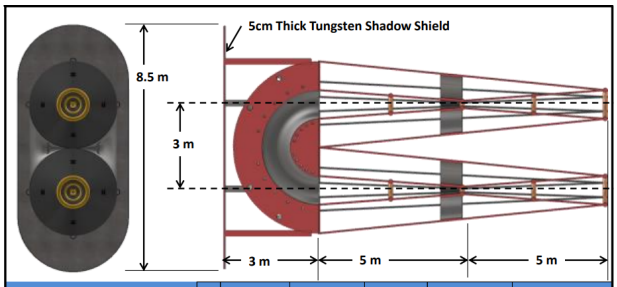

Fission Fragment MEL	Qty	Unit Mass (kg)	Basic Mass (kg)	MGA (%)	MGA (kg)	Predicted Mass (kg)
2.0 Propulsion			222709	21%	46198	268907
2.1 Moderator	1	70260	70260	30%	21078	91338
2.2 Core Heat Shield	1	8000	8000	30%	2400	10400
2.4 Core Superconducting Magnet Assembly	1	31062	31062	30%	9319	40381
2.5 Engine Structure	1	7026	7026	30%	2108	9134
2.6 Nozzle Structure	2	2073	4147	30%	1244	5391
2.7 Nozzle Magnet Assembly	2	2250	4500	30%	1350	5850
2.8 Dust Injector	1	2000	2000	30%	600	2600
2.9 Shadow Shielding	1	25000	25000	30%	7500	32500
2.10 Control Drums	1	500	500	30%	150	650
2.11 Hydrogen Pumps	10	50	500	30%	150	650
2.12 Hydrogen Feed/Injector Assembly	2	500	1000	30%	300	1300
2.13 Tanks	5	13743	68714	0%	0	68714

(a)

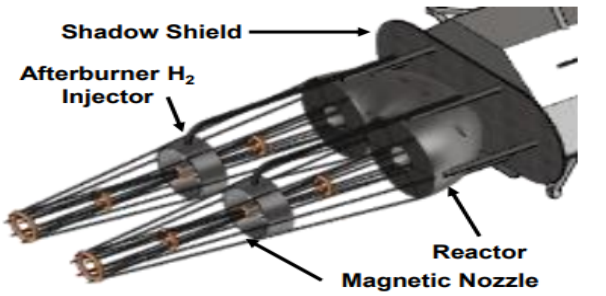

(b)

Fig. 7 (a) Half-torus FFRE with afterburner addition. The table lists the masses of components. Total mass of the engine with afterburner is predicted to be approximately 269 metric tons. Over a third of the mass is from the deuterated-^{13}C moderator. The dry-mass of the FFRE (without moderator) and excluding external tanks is about 109 metric tons, which can be launched by a heavy-lift vehicle such as SLS or Starship. (b) Another diagram of FFRE with afterburner displaying some components and an example of performance. The I_{sp} decreases to 32,000 seconds, but thrust increases to 4651 N. Both figures taken from [1].

Table 1. Masses from the fission event in Eq.1

	Mass [amu]	Mass $\left[10^{-25}\text{kg}\right]$
Neutron	1.0087	0.0167
$^{242\text{m}}$Am	242.0595	4.0195
^{100}Mo	99.9075	1.6590
^{140}I	139.9310	2.3236
Reactants Total	243.0682	4.0362
Products Total	242.8639	4.0329
Difference	0.20439	0.00339

be presented.

A. Basic Physics of the Fission Fragment Rocket Engine

As previously discussed, the whole idea of the FFRE is situated around directly expelling the products of nuclear fission reactions to produce thrust. Thus, the first step in analyzing engine performance should come from the fission events themselves. Currently, the most promising nuclear fuel is $^{242\text{m}}$Am, primarily due to its high thermal neutron cross section; it will be considered for this analysis.

Neutron-induced fission events typically result in two atomic species of roughly half the atomic number of the parent species. Experiments monitoring neutron-induced fission of ^{241}Am show this to be the case with products ranging from Zirconium (Z=40) to Europium (Z=63) [13]. Let's consider the example of Molybdenum and Iodine fission products with 3 neutrons being ejected. We have the reaction:

$$ {}^{1}_{0}\text{n} + {}^{242m}_{95}\text{Am} \longrightarrow {}^{100}_{42}\text{Mo} + {}^{140}_{53}\text{I} + 3\,{}^{1}_{0}\text{n} \tag{1} $$

Note that this reaction may or may not be realistic (I am not a chemist), but it is sufficient for the example. Of course, the sum of the mass of the products (including neutrons) will not equal that of the reactants. This difference in mass is expressed as the energy released by the fission event given by $E = mc^2$. The masses involved in this fission event are listed in Table 1.

The resulting mass defect of 3.39406×10^{-28} kg translates to a released energy of 3.05042×10^{-11} J, or ~ 190.4 MeV. This is consistent with other nuclear fission reactions such as uranium-235 which releases about 200 MeV per fission.

A majority of the energy that is released is in the form of kinetic energy of the fission fragments and the separated neutrons. The remaining energy takes the form of gamma rays, beta particles, or neutrinos. Let's assume that 80% of the released energy (152.32 MeV) is evenly split between the kinetic energy of the fission fragments. That is, both the ^{100}Mo and ^{140}I atoms have a kinetic energy of 76.16 MeV. Simply re-arranging the equation $KE = \frac{1}{2} m_{ff} v_{ff}^2$, we can find the ejection velocities of the fission fragments (see Table 2). It should be noted that the force that accelerates the fragments to such high velocities is Coulomb repulsion. After the perturbed parent nucleus splits, the resulting fragments then obtain their own electric charge, but remain only femtometers away from one another causing them to experience a strong repulsion force. It may be more accurate to use electrostatics to determine the fragments' velocities, but again, the present analysis should remain adequate.

The resulting velocities are a few percent the speed of light which entails specific impulses greater than 1,000,000 seconds, just as claimed by George Chapline [4]. However, these values are representative of an ideal scenario – theoretical maximums. In reality, most fragments will not take direct paths out the back of the engine. Most fragments should be capable of escaping the dusty plasma cloud (see Fig. 2), but that does not mean there will be no interactions between escaping fragments and the rest of the cloud. The particles are also being redirected out the nozzle by the magnetic mirror; though, because magnetic fields do no work, it can not change the kinetic energy of the fragments. Ultimately, the speeds at which the fragments exit the nozzle will be only a fraction of their initial speed. Recall that

Table 2. Theoretical fission fragment velocities

	v_{ff} $\left[10^7 \text{m s}^{-1}\right]$	% c	I_{sp} $\left[10^6 \text{sec}\right]$
^{100}Mo	1.3560	4.25	1.3823
^{140}I	1.1457	3.82	1.1679

Note. — The FFRE is designed to operate in a vacuum, so the fission fragment exit velocity (v_{ff}) is equivalent to the effective exhaust velocity of the engine; thus, I_{sp} is simply the fragment velocity divided by Earth standard gravity.

Table 3. Reduced fission fragment velocities

	v_{ff} $\left[10^6 \text{m s}^{-1}\right]$	% c	I_{sp} [sec]
^{100}Mo	5.4239	1.81	552, 901
^{140}I	4.5831	1.53	467, 185
Average	5.0035	1.67	510, 043

Note. — Fission fragments that exit the nozzle of the FFRE will likely not have the theoretical values displayed in Table 2. They will be slowed by the dusty plasma cloud as they exit and, thus, will escape the engine and contribute to thrust with a fraction of their initial velocity. This table displays a 40% reduction in velocity compared to Table 2.

switching the nuclear fuel from uranium or plutonium to americium increased the fraction of fragments contributing to thrust to 40% while the remaining 60% generated heat in the core. Let's make the assumption that the fragments that do contribute to thrust do so with 40% their initial fission speeds (see Table 3). When taking this into consideration, the outcome is nearly identical (relatively) to the tuna can iteration of the FFRE which had an I_{sp} of 527,000 seconds (Figure 5).

The next variable that should be investigated is the thrust of the engine. Calculating thrust requires knowledge of the mass flow rate of the propellant – the fission fragments. This, in turn, depends on the rate at which the nuclear material fissions, or the power of the reactor. The tuna can FFRE was slated to generate 1000MW of power with, according to [1], 111MW of power escaping the reactor in the form of fragments. We can use the relationship between force and power

$$F_t = \frac{P_{jr}}{v_{ff}} \tag{2}$$

and the thrust equation

$$F_t = \dot{m} v_{ff} \tag{3}$$

to obtain an estimate of the jet mass flow rate

$$\dot{m} = \frac{P_{jr}}{v_{ff}^2} = \frac{1.11 \times 10^8 W}{\left(5.0035 \times 10^6 \text{ m s}^{-1}\right)^2} = 4.4338 \times 10^{-6} \text{ kg s}^{-1} = 0.0044 \text{ g s}^{-1} \quad (4)$$

This mass flow rate give a thrust of 22.18 N. These values are off by a factor of 2 as compared to [1]; with 111MW of jet power, the tuna can geometry had a mass flow rate of 0.008 grams per second and a thrust of 43 N (Fig. 5)

Similar analyses can be conducted for the half-torus geometry FFRE – without the afterburner, the exhaust velocity and specific impulse should remain mostly unchanged. The thrust would increase by a factor of approximately 2.5 due to the greater power output from 1000 MW to 2500 MW (assuming the jet power scales linearly with reactor power) in addition to the two exhaust ports. That is: $I_{sp} = 510,043$ sec, $P_{jr} = 111MW * 2.5 = 277.5MW$ gives a mass flow rate of $\dot{m} = 0.0111$ gm s^{-1} and thrust $F_t = 55.46$ N.

However, according to Figure 7b, the mass flow of fission fragments for the half-torus is 0.031 gm s^{-1} which is ~ 2.8 times greater than the value calculated here and ~ 3.88 times greater than the tuna can flow rate of 0.008 gm s^{-1}. Using $\dot{m}$ given by [1] (0.031 gm s^{-1}) and the exhaust velocity calculated in Table 3 gives the half-torus FFRE (without afterburner) a thrust of $F_t = 155.11$ N. While the thrust of the half-torus configuration is higher than the tuna can, one must account for the increase in engine mass which effects the engine's acceleration (without considering the mass of the rest of the spacecraft). The most significant sources of engine mass come from the amount of moderator material surrounding the core and the superconducting magnet that generates the magnetic mirror. The amount of moderator material increases from approximately 51.2 metric tons to 91.34 mT and the magnet mass increases from 28.5 mT to 40.38 mT. Overall, the FFRE tuna can mass is estimated to be 113.4 mT and the half-torus mass (not including the afterburner structure mass) is 187 mT (see Figs. 3b & 6). Using the equation $F_t = m_e a_e$, the base acceleration of the tuna can is $a_e = 3.79 \times 10^{-4}$ m s^{-2} while the half-torus is still higher at $a_e = 8.29 \times 10^{-4}$ m s^{-2}.

Now, let's consider a the half-torus configuration including the afterburner. This analysis will not derive the momentum transfer of the fragments to the injected hydrogen. Instead, it will use the values given in Figure 7. The afterburner nozzle assembly, and supporting hydrogen-structures (pumps, 5 holding tanks) add about 82 mT to the engine with 84% of that mass coming from the hydrogen storage tanks. The mass of a single hydrogen tank is only 13.7 mT. Of course, the mission-design and target body of the FFRE spacecraft will determine the amount of hydrogen fuel mass and number of tanks required. Similarly, the afterburner performance can be altered by the amount of hydrogen injected into the fission fragment exhaust beam which can be optimized for each mission; this analysis is not included but sticks to the configurations given by [1] and Figure 7 which uses 5 hydrogen tanks. The specific impulse of 32,000 seconds implies an average fragment exit velocity of 313,920 m s^{-1}. The injected hydrogen mass flow rate is given as 18 grams per second which increases the half-torus mass flow rate from 0.031 gm s^{-1} to 18.031 gm s^{-1} of combined hydrogen and fission fragments. This should produce a thrust of 0.018031 kg s^{-1} * 313,920 m s^{-1} = 5660.29N, though the thrust value given in Figure7 is 4651 N. I am probably forgetting something or missing a nuance to how the engine setup and mass injection affects the thrust. With a total mass of 269 mT, the afterburner FFRE here would produce a base acceleration of $a_e = 1.73 \times 10^{-2}$ m s^{-2}.

Table 4 presents a summary of the FFRE performance for the tuna can, half-torus, and half-torus afterburner configurations. While the performance values derived from an example fission event of ^{242m}Am produces similar results to those of the original NIAC study [1], they are not exact, and they are not meant to. The calculations here are to give the reader a general idea of where the performance values of the FFRE originate. Therefore, to maintain consistency and accuracy, the data presented in Table 4 are mostly from [1] and Figures 5 & 7, though hopefully with a little more context and understanding of where they come from.

B. Mission Analysis

This (sub)section presents a mission of an interplanetary spacecraft utilizing the afterburner FFRE configuration. The spacecraft itself is nearly identical to version 2 of the 'New Discovery' vehicle presented in [1] and shown in Figure 8. The original (version 1) concept of New Discovery used the tuna can FFRE (Figure 3b) and was designed to travel to Jupiter's moon, Callisto. It was heavily influenced by the conceptual Human Outer Planet Exploration (HOPE) mission designed by NASA in 2003 [14]. Version 2 of the spacecraft uses the afterburner configuration of the FFRE for a mission to Mars (Figure 8b).

The example mission analyzed here is a mix between the two previously investigated missions to Jupiter and Mars. A nearly identical spacecraft to version 2 of New Discovery is considered for a journey to Saturn and back.

Table 4. FFRE Performance Analysis

Engine Configuration	Dry Mass* [mT]	Dry Mass† [mT]	P_{jr} [MW]	Total $\dot{m}$ $\left[\text{kg s}^{-1}\right]$	I_{sp} [sec]	F_t [N]
Tuna Can	62.2	113.4	111	8×10^{-6}	527,000	43
Half-Torus	95.67	187	277.5 (?)	3.1×10^{-5}	527,000	160
Afterburner Half-Torus	108.86	268.91	277.5 (?)	1.8031×10^{-2}	32,000	4651

Note. — The performance values in this table are taken or interpreted from [1] and Figure 7. While the basic analysis conducted in this section, originating from the fission of ^{242m}Am, produce similar performance values as [1], they are not rigorous. So, this table uses the information from the source. Wet mass of the engines are not included because the amount of fuel will vary with the mission design. The jet power (P_{jr}) is given for the tuna can, but assumed for the half-torus geometries, hence the question mark.

* Dry mass *without* moderator mass; for the afterburner configuration this dry mass excludes moderator material *and* hydrogen tank mass.

† Mass of the engine *with* moderator material, but *without* fuel mass; for afterburner, this dry mass includes the moderator material and the mass of 5 hydrogen tanks, but without the actual fuel mass.

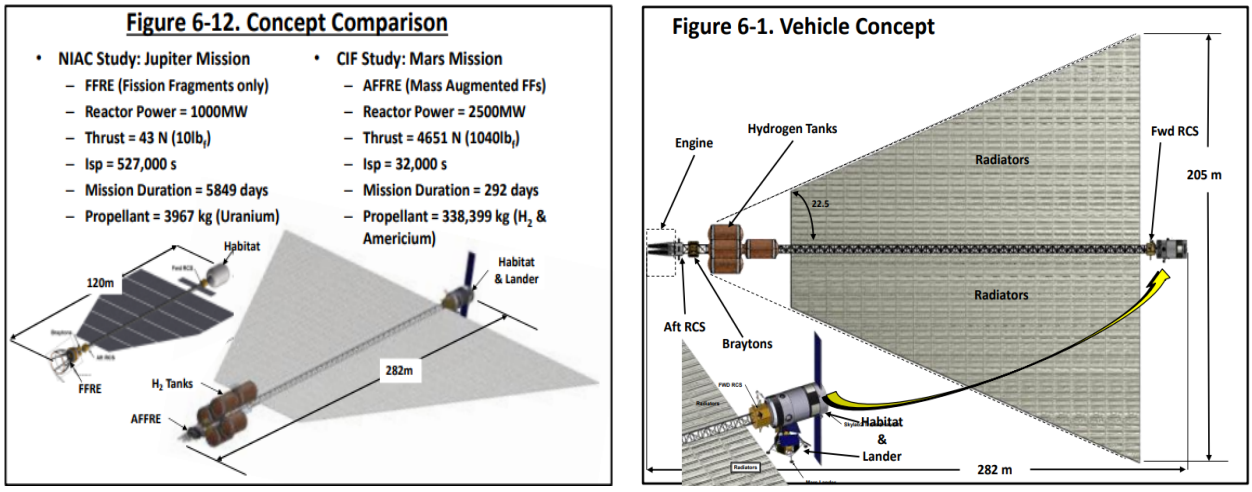

(a) **(b)**

Fig. 8 (a) *Left:* The original 'New Discovery' spacecraft which used the tuna can FFRE for a mission to Callisto. *Right:* Version 2 of New Discovery'which uses the afterburner FFRE for a mission to Mars. (b) More detailed of version 2. Because the power output increases from 1000 MW to 2500MW, the amount of radiator area required increases, ultimately increasing the size of the ship. Taken from [1].

1. A Brief Explanation of Kerbal Space Program and its Utility for Real Mission Analysis

In order to design and optimize a trajectory to Saturn from Earth, the software "KSP Trajectory Optimization Tool" (KSPTOT) is used. This software was originally created to help design missions and optimize spacecraft trajectories within the well-known space-program simulator video game Kerbal Space Program (KSP). While one may be tempted to shrug off the legitimacy of using a video game to design a mission, this assumption would be one made in ignorance. KSP is, at its core, a space-mission simulator. The setting is within a fictional solar system that is only a fraction of the size of reality, but this is simply for gameplay-mechanics purposes. The game still implements rocketry, physics (including thermal and aerodynamics), and astrodynamics just as any computer simulation of a space-mission would. There is plenty of documentation on the physics engines and technicalities of KSP online.

Where the game becomes useful to real-life mission design is with the implementation of "mods." Mods are modification to the game which can be created and used by anyone who owns the game. Mods exist that convert the in-game solar system into simulations of our real solar system as well as overhauling many parts of the game to more closely imitate real life. This, along with a few other mods, essentially convert the KSP videogame into a computational simulation tool that can be used for realistic mission design and analysis. The primary mods used for this realism overhaul of KSP are, aptly named, 'Realism Overhaul' [15] and 'Real Solar System' [16].

KSPTOT can be used in tandem with these realism-mods to generate and optimize missions similar to real life. It should be noted that this method of mission design was not my first instinct: I attempted to use NASA's Evolutionary Mission Trajectory Generator, though to say that the process of getting it to work was not a user-friendly experience would be an understatement. Secondly, I attempted to use NASA's General Mission Analysis Tool. This was more successful, but has quite a steep learning curve. Finally, as a last resort, I looked to KSP and discovered KSPTOT (in addition to the realism mods) which is extremely user friendly, is well documented, and is based in real physics, astrodynamics, and uses officially licensed optimization algorithms.

KSPTOT has proved to be a useful and powerful software for mission design and optimization which can be applied to real life.

2. The Mission

KSPTOT assumes all maneuvers are impulsive. Because of the relatively low-thrust of the afterburner FFRE, multiple finite duration burns will be necessary to attain Δv's to perform maneuvers. The spacecraft for this mission has a 'dry mass' of 740 mT; in this case, dry mass refers to all mass that is not ^{242m}Am or hydrogen fuel. There is 400 mT of fuel. This gives a total initial spacecraft mass of 1140mT.

It is assumed that whenever the engine is fired, it always does so with the same performance parameters. The mass ratio of hydrogen-to-fission-fragments is equal to the mass flow rates displayed in Figure 7b:

$$\frac{H_2}{FF} = \frac{1.8 \times 10^{-2}\ \mathrm{kg\,s^{-1}}}{3.1 \times 10^{-5}\ \mathrm{kg\,s^{-1}}} = 580.645 \tag{5}$$

Specific impulse is considered constant at 32,000 seconds and when firing, the thrust is 4651N. The spacecraft is assumed to begin in a circular orbit around Earth with a semi-major axis of 7500 km and inclination of 30 degrees. The mission is set to begin in 2030.

First, KSPTOT can be used to find the optimal transfer window between Earth and Saturn using porkchop plots. Understanding the date format of the code is a bit tricky, but I will explain it here. The KSP realism mods set the initial epoch of the game to be January 1, 1951. KSPTOT denotes this date as 'Year 1, Day 1.' Unfortunately (for dispaying time in years and days), KSPTOT does not use a calendar, but counts seconds and divides by 365 to convert to years and days. The primary issue with this is that it neglects the extra day in leap years. The time set under 'Earliest Departure Time' in Figure 9 is 2493072000 seconds past January 1, 1951. On a calendar, this puts the date as January 1, 2030. However, the date displayed by KSPTOT is Year 80, Day 21. If strictly counting up from 0 (January 1, 1951 = Year 0, Day 1), this would be January 21, 2031. Those 21 extra days are from leap years. While this is slightly annoying to us, it does not actually impact the results or timing of the code because it keeps track of time by counting seconds.

Anyway, considering January 1, 2030 as the earliest transfer window, it finds an efficient transfer which occurs with departure from Earth on August 12, 2030 and arrival on June 6, 2035 requiring a combined departure plus arrival Δv = 16.552 km s^{-1} (see the text box at the bottom of Figure9a instead of the box in the middle).

However, this is just a general analysis used to find a good transfer window. Using this as a sort of starting point, specific maneuvers can be created. First, the trans-Saturn injection (TSI) burn which is displayed in Figure 10, is developed. This maneuver allows the spacecraft to escape Earth's gravity and enter into an elliptical orbit about the Sun that will intercept Saturn along the way. This maneuver has a Δv requirement of 7.735 km s^{-1}.

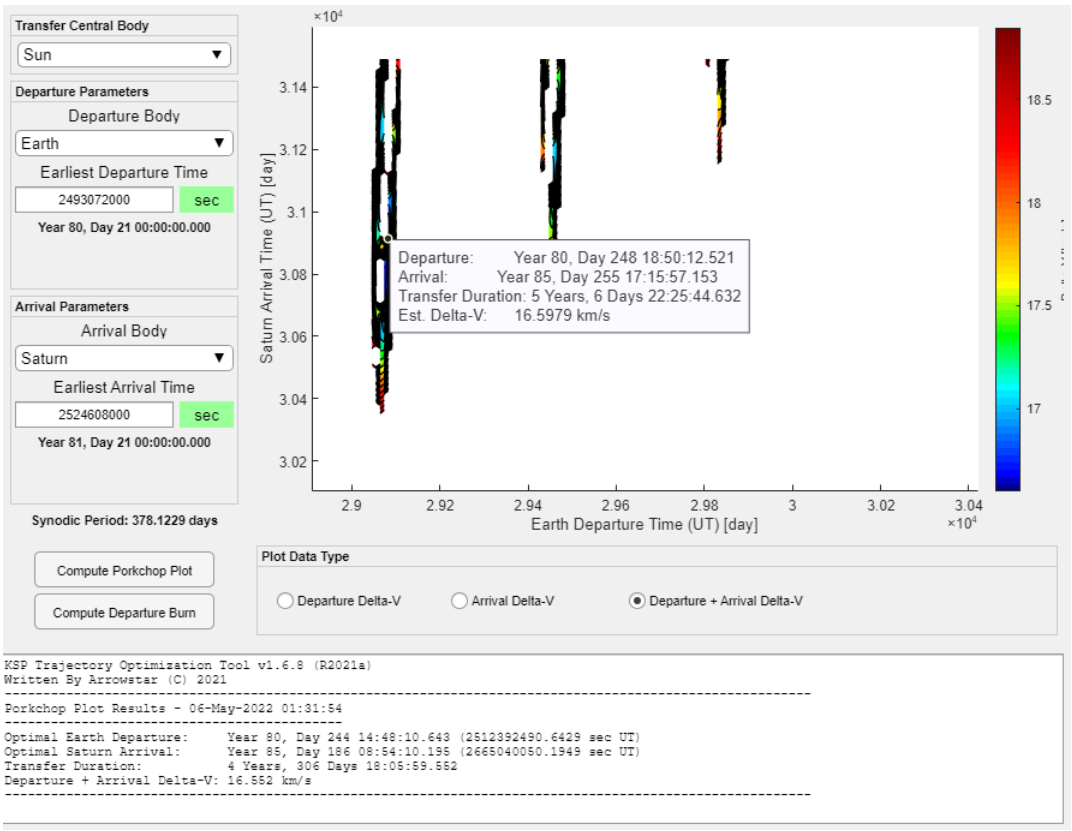

(a)

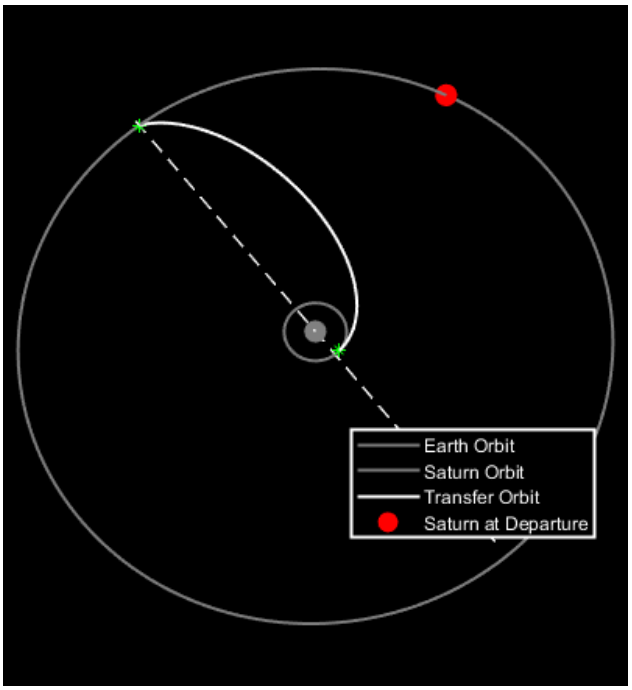

(b)

Fig. 9 (a) KSPTOT's calculation of an efficient transfer from Earth to Saturn considering times past January 2030. The format of the time (Year 80...) is simply due to the realism mods. The Real Solar System mod sets the initial epoch of the game (and, thus, simulations) as January 1, 1951. KSPTOT considers this Year 1, Day 1. Unfortunately KSPTOT does not count leap days, so as time progresses, the 'Year, Day' format becomes more inaccurate. One can count seconds beyond 1/1/1951, however to get accurate times (which is what the software actually does). Thus, Year 80, Day 21 corresponds to January 1, 2030. The found transfer (see text at the bottom of the figure) would take 4.84 year and requires a combined departure plus arrival Δv = 16.552 km s^{-1}. (b) A depiction of the transfer.

We can use the Tsiolkovsky rocket equation to calculate the amount of fuel that must be expended during any of the maneuver burns. The rocket equation is

$$\Delta v = v_e \ln \frac{m_0}{m_f} \tag{6}$$

which can be rearranged for m_f and subtracted from m_0 to determine the amount of fuel required to complete the burn:

$$m_f = m_0 e^{-\Delta v / v_e} \tag{7}$$

Before the initial burn, the spacecraft mass is 1140 mT. Thus, for a 7.735 km s^{-1} burn,

$$m_f = (1.14 \times 10^6 \text{kg}) e^{-\frac{7735.29 \text{m s}^{-1}}{32{,}000 \text{s} * 9.81 \text{m s}^{-2}}} = 1112252.57 \text{kg} \tag{8}$$

So, the amount of fuel expended to enter the Earth-Saturn transfer orbit is $m_0 - m_f = 1140\,\text{mT} - 1112.252\,\text{mT} = 27.748\,\text{mT}$. With the H_2-to-FF mass ratio of 580.645, this means that approximately 47.788 kg of ^{242m}Am and 27.7002 mT of H_2 are used.

The coast between Earth and Saturn takes approximately 1736 days. The Saturn-insertion burn places the spacecraft in an eccentric orbit about Saturn with semi-major axis of 489,030.8 km, eccentricity = 0.4083, negligible inclination, ascending node of 350.8 degrees and argument of periapse of 25.53 degrees. This orbit is intentionally left non-circular to allow for better overall access to all of Saturn's moons. Figure 11 shows the spacecraft's coast to Saturn and it's resulting orbit after the insertion maneuver. The Δv required to insert the spacecraft into this orbit is 6577.7 m s^{-1}. Solving again for the amount of fuel required, though now using $m_0 = 1112.252\,\text{mT}$ gives a final spacecraft mass of $m_f = 1089.19\,\text{mT}$, thus the total amount of fuel expended is 23.063 mT. That corresponds to 39.65 kg of ^{242m}Am and 23.0234 mT of H_2.

The spacecraft will remain at Saturn for approximately 308 days, or about 75 orbits around Saturn. This duration is chosen arbitrarily. In reality, at this point, there would likely be a large jettison of mass due to the deployment of a lander, rover, or other scientific instruments, though this is not modeled. The dry mass of the spacecraft remains constant through the entire mission at 740 mT. The only mass being lost is that of the spent fuel.

Finally, the mission departs Saturn on a transfer orbit back to Earth which requires a Δv of 7989.1 m s^{-1}, or 47.06 kg of ^{242m}Am and 27.323 mT of H_2. The insertion back into Earth orbit is, by far, the most energy intensive maneuver. Including insertion, circularizing, and (slightly) decreasing the inclination of the orbit around Earth requires a total Δv of 17949.8 m s^{-1}. This is achieved by burning 59 mT of fuel; 101.5 kg of americium and 58.91 mT of hydrogen. Thus, the final mass of the spacecraft is 1002.81 mT. Saturn departure, Earth insertion, and the full mission trajectory are shown in Figure 12. A summary of the mission is given in Table5. The total spacecraft mass over the course of the mission is shown in Figure 13. This analysis makes clear that the FFRE is an extremely efficient engine requiring less than 300 kg of nuclear fuel and about 1.5 space shuttle external tanks worth of liquid hydrogen for a mission to Saturn. No staging of the spacecraft is required. Theoretically, it could be refueled, serviced for any repairs, and begin a new mission not long after its return.

VI. Conclusion

The fission fragment rocket engine is a nuclear reactor exposed to a vacuum allowing fission products to escape out a magnetic nozzle in order to produce thrust. Because fission fragments are launched at speeds a few percent the speed of light, extremely high specific impulses are achievable, however with only a few newtons of thrust. By including an afterburner which injects liquid hydrogen into the fission fragment exhaust beam, the thrust can be increased for a trade-off in specific impulse. In addition, the FFRE heat generated by the nuclear reactor can be harnessed to generate power for the extire spacecraft. Much of the limitations of the engine are not related to pressure, but rather thermal management. A vast majority of the heat generated by the core must be dumped into space via radiators.

An example mission analysis was presented of a FFRE powered spacecraft travelling to Saturn and back in 15 years. It was capable of doing so without staging and using approximately 137 metric tons of fuel: 99.86% of that mass being composed of hydrogen and less than 300 kg being the nuclear fuel americium-242m. Once the spacecraft has returned to Earth, it should be capable of being reused. Thus, the FFRE is not only efficient in terms of propulsion, but in the long term would become increasingly cost effective the more it is re-used, similar to SpaceX's Falcon 9.

The FFRE has been the subject of a few studies, mostly by the same team of researchers at NASA Marshall Space Flight Center. It was funded for an NIAC phase I study in 2012, but never made it further than that. The FFRE is

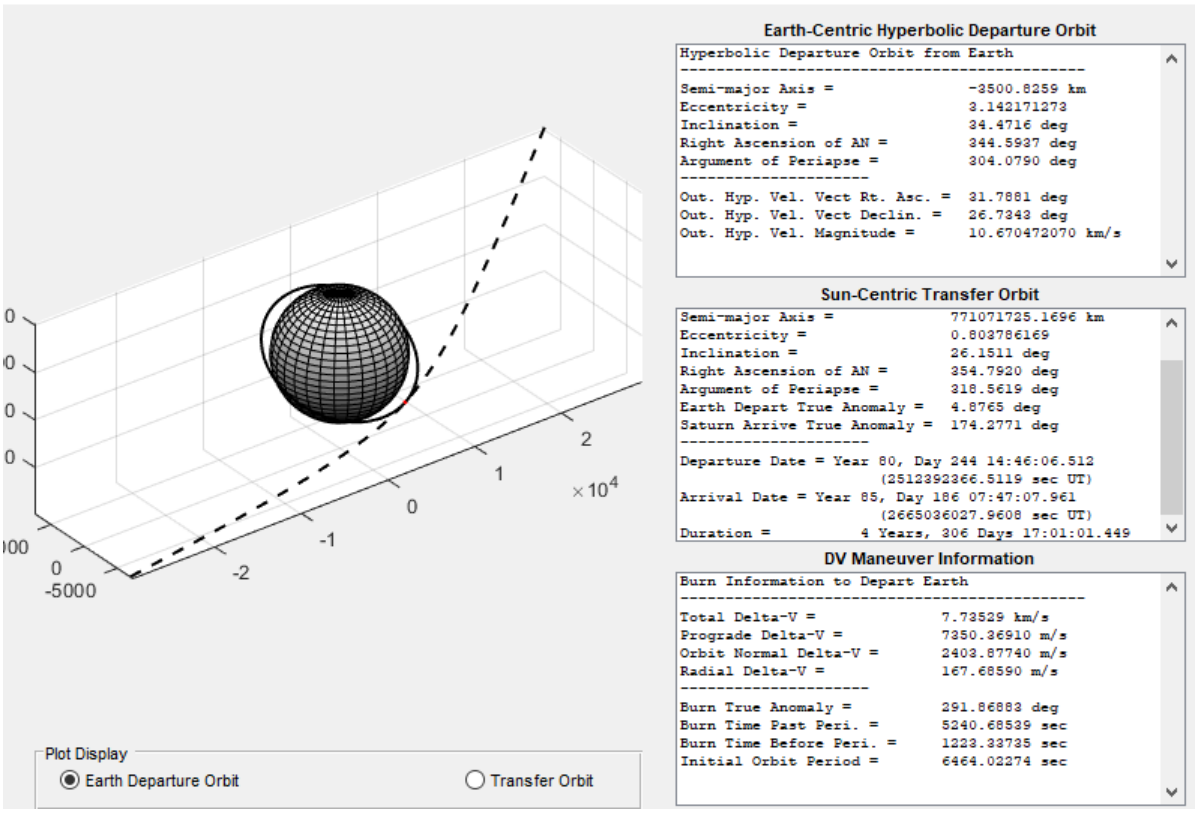

(a)

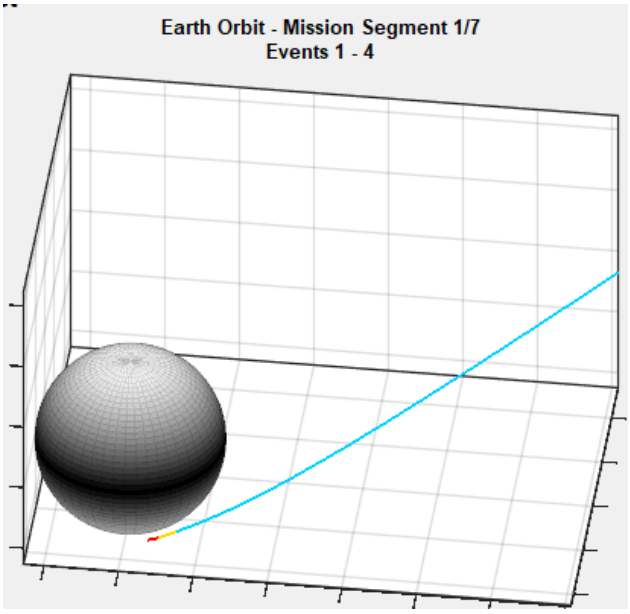

(b)

Fig. 10 (a) Orbital and maneuver parameters to depart Earth and enter a transfer orbit to Saturn. The important piece of information is the total Δv required in the bottom box. (b) A segmented view of the departure from Earth. The red is the motion of the spacecraft on its initial parking orbit around Earth just before departure. The yellow segment is the maneuver burn. The blue is the resulting trajectory. KSPTOT assumes burns are impulsive, so in reality, an FFRE powered spacecraft would need to burn many times over many orbits to escape Earth.

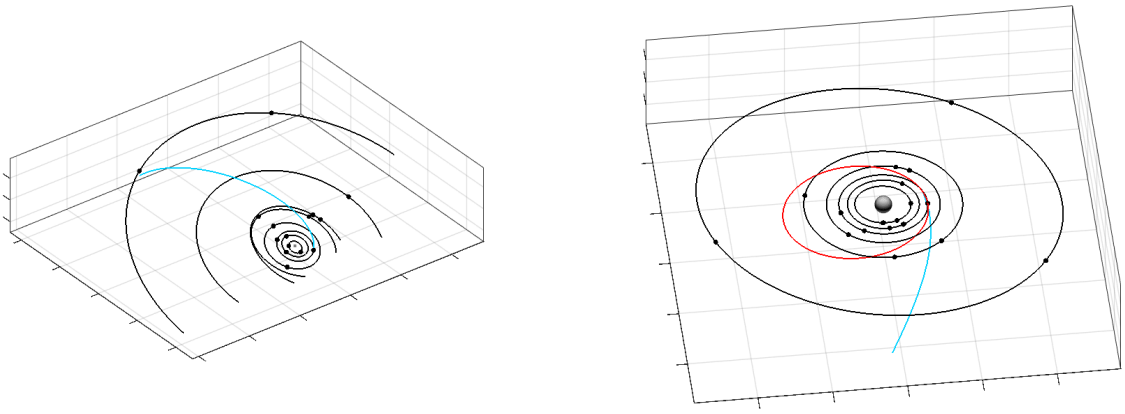

(a) **(b)**

Fig. 11 (a) The coast from Earth to Saturn. This takes approximately 1736 days. The orbits shown from furthest out moving inwards is Saturn, Jupiter, Vesta and Ceres, Mars, Earth, Venus, Mercury, and the Sun is the center. (b) A view of the parking orbit about Saturn (red) after the coast phase. The orbits of Saturn's moons from furthest out to closest in are Titan, Rhea, Dione, Tethys, Enceladus, and Mimas.

Table 5. Example Mission Summary

Event	Δv [km s^{-1}]	^{242m}Am Used [mT]	H_2 Used [mT]	Total S/C Mass [mT]	Time of Event [Days]
Initial State	135.655	0.6877	399.312	1140	0
Earth Departure	7.735	0.0478	27.700	1112.252	1
Saturn Insertion	6.578	0.0397	23.023	1089.188	1736
Saturn Departure	7.989	0.0471	27.323	1061.819	2044
Earth Insertion	17.950	0.1015	58.909	1002.808	5487
Totals	40.252	0.2361	136.955	137.192	5489

Note. — The initial state shows the total possible Δv of the spacecraft, the initial masses of fuel, and the initial mass of the entire spacecraft. The 'Totals' row sums up the Δv of the entire mission, and the amount of fuel used (236.1 kg of Americium, 136.955 mT of hydrogen combine for 137.192mT of fuel expended). Thus, the mission had 451.6 kg of Americium and 262.357 mT of Hydrogen left over. This implies that the initial amount of fuel should be reduced a bit, though still leaving some extra fuel as a safety margin. The total round-trip mission takes just of 15 years.

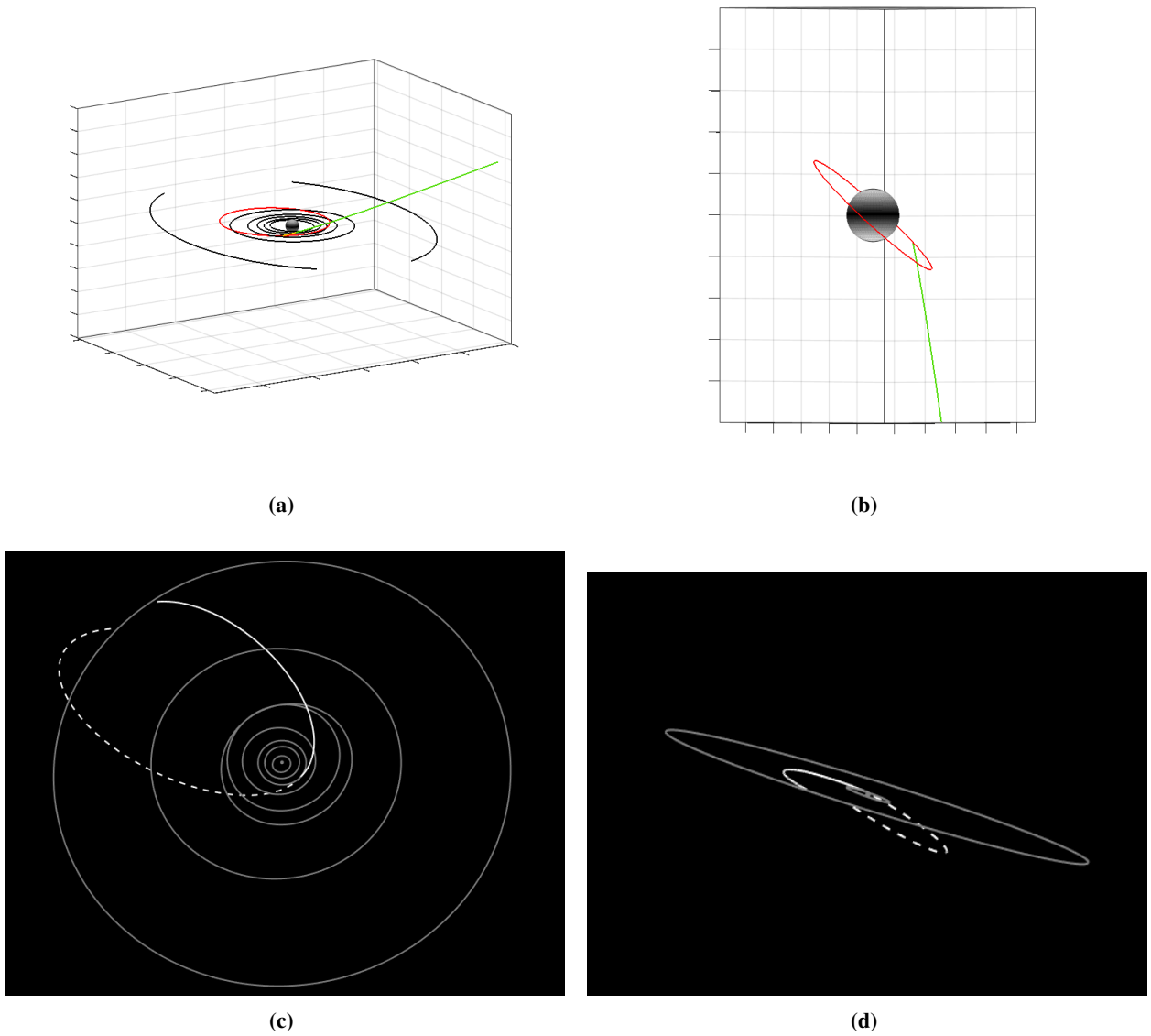

Fig. 12 (a) Departure from Saturn. The red is the parking orbit around Saturn, the yellow is the (impulsive) burn, and green is the outbound trajectory back to Earth. (b) The Earth-insertion burn is quite dramatic, requiring approximately 18 km s^{-1} of Δv. The orbit is circularized, but remains quite inclined due to the steep angle of incidence. This, of course, can be adjusted with subsequent burns, though it is not included here. At this point, the mission would be over. (c) The coast to Saturn from Earth (solid) and the coast from Saturn back to Earth (dotted). (d) The mission trajectory as seem form edge on to give more insight in to the out-of-plane motion of the mission. Only the orbits of Saturn and Earth are shown to prevent clutter. The solid line is going from Earth to Saturn and the dotted line is returning to Earth.

compatible with current physics and much of the technology required to build one already exists. That is not to say that there are no hurdles in its path, but it is not as 'far-future' a technology as one might think. Given funding for research and development, an engineering model and possibly a functional unit could likely be developed within the next 20-30 years.

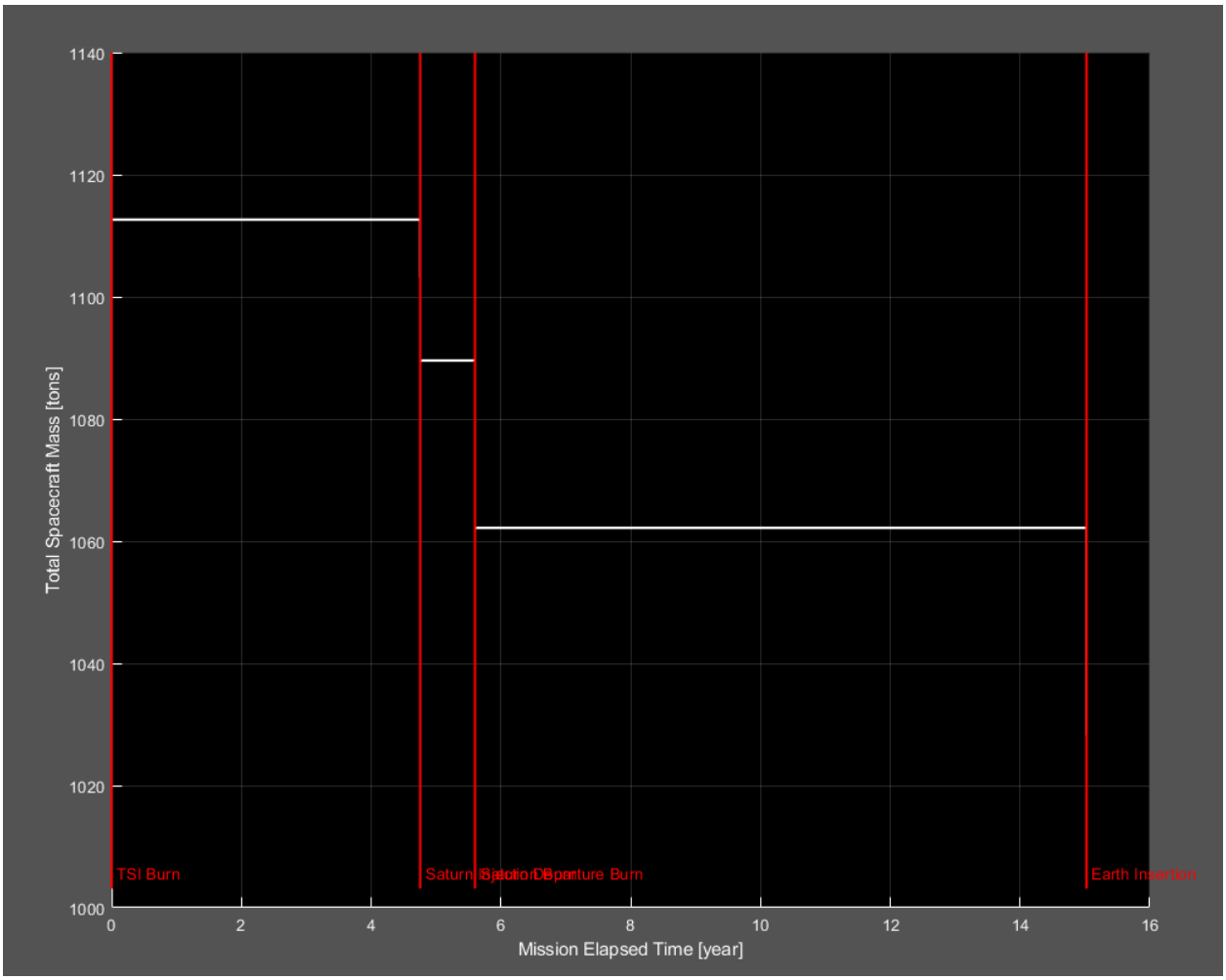

Fig. 13 Mass of the spacecraft over the course of the mission. The vertical lines represent events in the mission. TSI stands for trans-Saturn injection. Over the 15 year, round-trip mission, the spacecraft uses approximately 137 mT of fuel decreasing the total mass from 1140 mT to 1003 mT. This mission ended up having much more fuel than was necessary. The software KSPTOT models maneuvers as impulsive. That is why the decrease in mass is non-continuous. Because the FFRE has relatively low thrust compared to chemical engines, the maneuvers would take longer as the engine must fire for longer periods of time. Thus, if maneuvers were modeled with finite-duration burns, the drop in mass would resemble more of downwards ramp with a few plateaus rather than stairs.

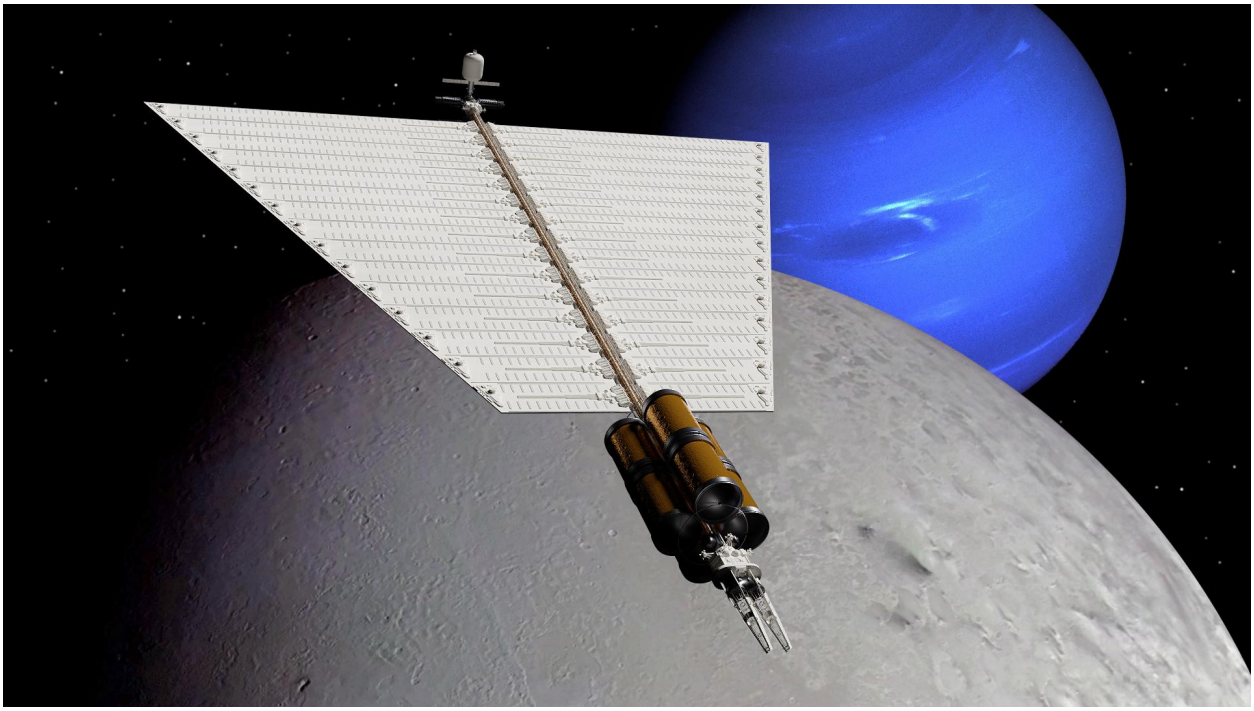

Fig. 14 Here is a pretty render of the FFRE by Tea Monster [17]

References

[1] Werka, R., Clark, R. L., Sheldon, R. B., and Percy, T., "Final Report: Concept Assessment of a Fission Fragment Rocket Engine (FFRE) Propelled Spacecraft," *FY11 NIAC Phase 1 Study*, 2012. URL `https://www.nasa.gov/sites/default/files/atoms/files/niac_2011_phasei_werka_ffre_tagged.pdf`.

[2] Clark, R. L., and Sheldon, R. B., "Dusty Plasma Based Fission Fragment Nuclear Reactor," *Proc. of 41st AIAA/ASME/SAE/ASEE JPC*, AIAA paper #2005-4460, 2005.

[3] Clark, R. L., and Sheldon, R. B., "A Six Component Model for Dusty Plasma Nuclear Fission Fragment Propulsion," *Nuclear and Emerging Technologies for Space*, American Nuclear Society, 2016.

[4] Chapline, G. F., "Fission Fragment Rocket Concept," *Nuclear Instruments and Methods in Physics Research*, Vol. A271, 1988, pp. 207–208.

[5] Chapline, G. F., Dickson, P. W., and Schnitzler, B. G., "Fission Fragment Rockets – A Potential Breakthrough," *EG and G Idaho, Inc., Idaho Falls (USA)*, 1988.

[6] Chapline, G. F., and Matsuda, Y., "Energy Production Using Fission Fragment Rockets," *Fusion Technology*, Vol. 20:4P2, 1991, pp. 719–722.

[7] Hensle, D., Barker, J. T., Barrett, J. S., Bowden, N. S., Brewster, K. J., Bundgaard, J., Case, Z. Q., Casperson, R. J., Cebra, D. A., Classen, T., Duke, D. L., Fotiadis, N., Gearhart, J., Geppert-Kleinrath, V., Greife, U., Guardincerri, E., Hagmann, C., Heffner, M., Hicks, C. R., Higgins, D., Isenhower, L. D., Kazkaz, K., Kemnitz, A., Kiesling, K. J., King, J., Klay, J. L., Latta, J., Leal, E., Loveland, W., Lynch, M., Magee, J. A., Manning, B., Mendenhall, M. P., Monterial, M., Mosby, S., Oman, G., Prokop, C., Sangiorgio, S., Schmitt, K. T., Seilhan, B., Snyder, L., Tovesson, F., Towell, C. L., Towell, R. S., Towell, T. R., Walsh, N., Watson, T. S., Yao, L., and Younes, W., "Neutron-induced fission fragment angular distributions, anisotropy, and linear momentum transfer measured with the NIFFTE fission time projection chamber," *Physical Review C*, Vol. 102:1, 2020.

[8] Ronen, Y., and Shwageraus, E., "Ultra-thin 242m Am fuel elements in nuclear reactors," *Nuclear Instruments and Methods in Physics Research*, Vol. A455, 2000, pp. 442–451.

[9] Benetti, P., Cesana, A., Cinotti, L., Raselli, G. L., and Terrani, M., "Americium 242m and its potential use in space applications," *Journal of Physics: Conference Series*, Vol. 41:161, 2006.

[10] Brown, L. C., "Direct Energy Conversion Fission Reactor – Annual report for the period August 15, 2000 through September 30, 2001," *General Atomics Report*, Vol. GA–A23877, 2002.

[11] Tarditi, A. G., A, G. J., H, M. G., and H, S. J., "Feasibility of Traveling Wave Direct Energy Conversion of Fission Reaction Fragments," *Proceedings of Nuclear and Emerging Technologies for Space*, 2013.

[12] Chung, W., "Engine List 2 – Fission Fragment Type," 2022. URL http://www.projectrho.com/public_html/rocket/enginelist2.php#affre.

[13] Shinohara, N., Hatsukawa, Y., Hata, K., and Kohno, N., "Measurement of Fission Product Yields from Neutron-Induced Fission of Americium-241," *Journal of Nuclear Science and Technology*, Vol. 36:3, 1999, pp. 232–241.

[14] Adams, R. B., Alexander, R. A., Chapman, J. M., Fincher, S. S., Hopkins, R. C., Philips, A. D., Polsgrove, T. T., Litchford, P. B. W., R J and, Statham, G., White, P. S., and Thio, Y. C. F., "Conceptual Design of In-Space Vehicles for Human Exploration of the Outer Planets," *NASA Technical Publication - 212691*, 2003.

[15] Kell, N., "Realism Overhaul," 2022. URL https://forum.kerbalspaceprogram.com/index.php?/topic/155700-1101-realism-overhaul-27-jul-2021/#:~:text=Realism%20Overhaul%20is%20a%20mod,is%20the%20mod%20for%20you!

[16] Kell, N., "Real Solar System," 2022. URL https://forum.kerbalspaceprogram.com/index.php?/topic/177216-18-real-solar-system-v1815-27-jun-2021/.

[17] Monster, T., "Fission Fragment Afterburner Rocket to the Outer Planets," 2022. URL https://forum.nasaspaceflight.com/index.php?PHPSESSID=si428gi6kcu2ob2ljk8fcbs8gk&topic=47704.msg1925080#msg1925080.